

# Modeling of efficient mode matching and thermal-lensing effect on a laser-beam coupling into a mode-cleaner cavity

N. Uehara, E. K. Gustafson, M. M. Fejer, and R. L. Byer<sup>1</sup>

Edward L. Ginzton Laboratory, Stanford University, Stanford, CA 94305-4085

## ABSTRACT

We describe the spatial mode-matching of a diode-pumped Nd:YAG laser to a ring mode-cleaner cavity with an efficiency as high as 99.8 %. Spatial-mode coupling including thermal-lensing effects in the cavity are analyzed.

**Keywords:** mode matching, optical cavity, thermal-lensing effect, gravitational wave detection.

## 1. INTRODUCTION

Advanced interferometric gravitational wave detectors will use a 100 watt cw single-frequency laser at 1  $\mu\text{m}$  to improve the detection sensitivity at high frequencies[1]–[3]. To maximize the interferometric contrast, a diffraction-limited beam is required. The optical beam transmitted by an optical cavity on resonance is both spectrally filtered and temporally filtered. This mode-cleaner cavity consists of a high finesse Fabry-Perot interferometer and is used immediately after the laser source to achieve the spatial mode quality and the reduction in intensity noise demanded by the gravitational wave interferometers. To develop a high transmission and high finesse mode-cleaner cavity, it is essential to use lowloss and high reflectance mirrors. These mirrors made by ion-beam sputtering, have an optical loss that is less than 100 ppm (0.01 %) compared with 200 ppm or more loss from a standard commercial mirror made by electron-beam evaporation. The lowest loss mirror at 1  $\mu\text{m}$  reported to date has a total loss of 6 ppm[4]. In the future thermal effects in the mode-cleaner cavity will become important, as the incident laser power is increased[5]–[8]. The cavity internal power will exceed 100 kW and mirror distortion due to absorption ( $\sim 1$  ppm) at the high-reflectance (HR) coating will reduce the laser-beam coupling and transmission efficiency of the cavity.

In this paper, we describe efficient spatial-mode coupling as high as 99.8 % to a ring mode-cleaner cavity, and calculate thermal-lensing effects on the mirror substrate. In section 2, mode-coupling efficiency is defined. In section 3, the thermal-lensing effects associated with surface heating on the HR coating multilayers are used to calculate the mode-coupling efficiency and phase front distortion in the transmitted beam. The experimental setup and the mode-coupling experiment are discussed in the sections 4 and 5, respectively and in section 6, the paper is summarized.

## 2. DEFINITION OF MODE-COUPLING EFFICIENCY

Assume an electric field incident on an optical cavity in  $(x, y, z)$  coordinates;

$$\Psi(x, y, z) = \psi_x(x, z)\psi_y(y, z) \quad (1)$$

where the electric field is expressed as a product of the amplitudes of horizontal ( $x$ ) and vertical ( $y$ ) directions. The incident electric field  $\Psi(\mathbf{r})$  can be expressed as a normal-mode expansion using the Hermite-Gaussian eigenmodes

---

<sup>1</sup>Further author information:

N.U.(correspondance): E-mail: uehara@loki.stanford.edu or noboru.uehara@msn.com

E.K.G.: E-mail: gustaf@ee.stanford.edu

M.M.F.: E-mail: fejer@ee.stanford.edu

R.L.B.: E-mail: byer@ee.stanford.edu

$u_{m,n}$  of the optical cavity as[9]–[11]

$$\psi_x(x, z) = \sum_{m=0}^{\infty} c_{x,m} u_m(x, z) \quad (2)$$

$$\psi_y(y, z) = \sum_{n=0}^{\infty} c_{y,n} u_n(y, z) \quad (3)$$

where  $c_{\alpha,p}$  ( $\alpha=x,y, p=m,n$ ) is the expansion coefficient which is given by

$$c_{\alpha,p} = \frac{\int_v \psi_{\alpha}(\alpha, z) u_p(\alpha, z) d\alpha dz}{\sqrt{(\int_v |\psi_{\alpha}(\alpha, z)|^2 d\alpha dz)(\int_v |u_p(\alpha, z)|^2 d\alpha dz)}} \quad (4)$$

and the spatial integration is carried out over the cavity mode volume. The spatial mode-coupling efficiency in a cavity TEM<sub>*m*n</sub> mode is defined by the absolute square of the coefficients as

$$\kappa_{mn} = |c_{x,m} c_{y,n}|^2 = \frac{\left| \prod_{\alpha} \int_0^{L_c} dz \int \psi_{\alpha}(\alpha, z) u_p(\alpha, z) d\alpha \right|^2}{\prod_{\alpha} \left( \int_0^{L_c} dz \int |\psi_{\alpha}(\alpha, z)|^2 d\alpha \right) \left( \int_0^{L_c} dz \int |u_p(\alpha, z)|^2 d\alpha \right)} \quad (5)$$

where  $L_c$  is the cavity length and  $\kappa_{mn}$  satisfies

$$\sum_{m,n=0,0}^{\infty} \kappa_{mn} = 1. \quad (6)$$

$\kappa_{mn}$  can also be expressed as a ratio of the coupled TEM<sub>*m*n</sub> mode power to the total power as

$$\kappa_{mn} = \frac{P_{mn}}{\sum_{i,j} P_{ij}} \quad (7)$$

and is called the mode-coupling efficiency. Experimentally we want to evaluate the mode-coupling efficiency to a fundamental cavity TEM<sub>00</sub> mode. Here we assume that the incident field is a Gaussian beam

$$\psi_p(\alpha, z) = \frac{1}{\sqrt{\pi} W_{\alpha}(z)} \exp\left(-\frac{\alpha^2}{W_{\alpha}^2(z)}\right), \quad (8)$$

$$W_{\alpha}^2(z) = W_{\alpha 0}^2 \left\{ 1 + \left( \frac{(z - z_{\alpha})}{z_{\alpha 0}} \right)^2 \right\}, \quad (9)$$

$$z_{\alpha 0} = \pi W_{\alpha 0}^2 / \lambda, \quad (10)$$

where  $W_{\alpha}(z)$  and  $W_{\alpha 0}$  are the beam radius at 1/e in amplitude and the beam radius at the waist position  $z=z_{\alpha}$ , respectively  $\lambda$  is wavelength. The cavity fundamental eigenmode is given by

$$u_0(\alpha, z) = \frac{1}{\sqrt{\pi} W_{\alpha,e}(z)} \exp\left(-\frac{\alpha^2}{W_{\alpha,e}^2(z)}\right), \quad (11)$$

$$W_{\alpha,e}^2(z) = W_{\alpha e 0}^2 \left\{ 1 + \left( \frac{z}{z_{\alpha e 0}} \right)^2 \right\}, \quad (12)$$

$$z_{\alpha e 0} = \pi W_{\alpha e 0}^2 / \lambda, \quad (13)$$

where  $W_{\alpha,e}(z)$  and  $W_{\alpha e 0}$  are the beam radius at 1/e of the amplitude and the beam radius of the cavity eigenmodes at the waist position  $z = 0$ , respectively. Here we assumed that eigenmodes in the  $x$  and  $y$  axes have beam waists at

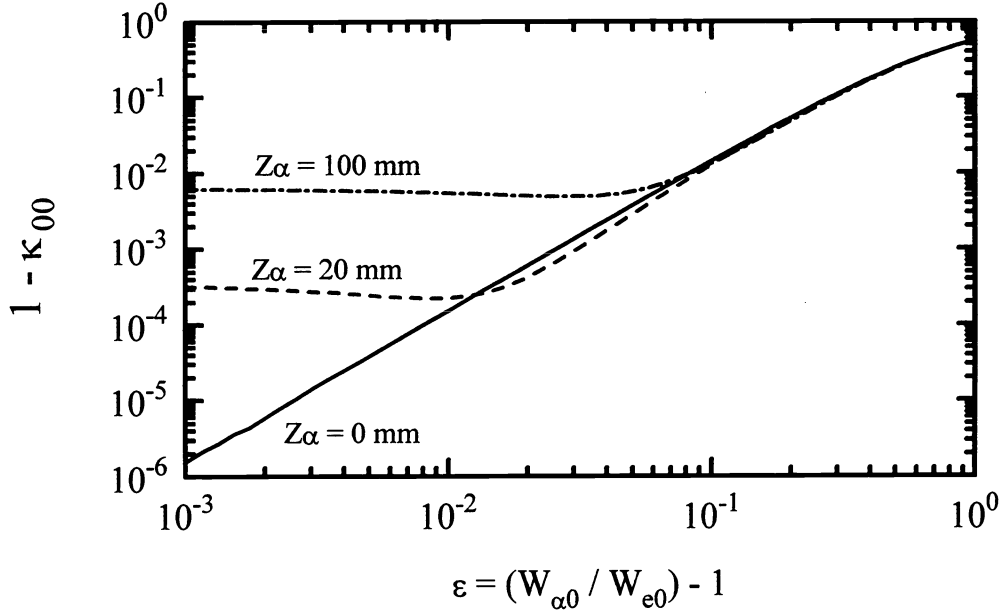


Figure 1: Calculated mode-coupling efficiency to a cavity  $TEM_{00}$  mode as a function of mode-size mismatch. Beam-waist radius of the cavity mode ( $W_{e0}$ ) and the cavity length ( $L_c$ ) are 0.372 mm and 200 mm, respectively. Relative beam-waist position ( $z_a$ ) of 0, 20 mm, and 100 mm are used and the laser wavelength is 1064 nm.

the same position ( $z = 0$ ). When both the incident field and the cavity eigenmode are Gaussian beams, the power mode-coupling efficiency to the cavity  $TEM_{00}$  mode in Eq. (5) simplifies to

$$\kappa_{00} = \frac{16 \prod_{\alpha=x,y} \left\{ \int_0^{L_c} \frac{1}{W_{\alpha}^2(z) + W_{\alpha,e}^2(z)} dz \right\}^2}{\prod_{\alpha} \left\{ \int_0^{L_c} \frac{1}{W_{\alpha}^2(z)} dz \right\} \left\{ \int_0^{L_c} \frac{1}{W_{\alpha,e}^2(z)} dz \right\}}. \quad (14)$$

We will now calculate some simple examples. Figure 1 shows a mode-coupling efficiency to a cavity fundamental mode as a function of mode-size mismatch defined by  $\epsilon = (W_{\alpha 0}/W_{e0}) - 1$  assuming cylindrical symmetry where the vertical axis is the mode-decoupling efficiency  $1 - \kappa_{00}$  assuming a laser wavelength, cavity waist size, and cavity length of 1064 nm, 0.372 mm, and 200 mm, respectively. These parameters are based on the ring mode-cleaner cavity discussed below. In the figure, waist-position mismatching of  $z_a = 0$  mm, 20 mm, and 100 mm are used. We find that waist-position mismatching is less sensitive than the mode-size mismatch. To achieve a mode-coupling efficiency ( $\kappa_{00}$ ) greater than 99 %, a mode-size mismatch and a waist-position mismatch to the cavity length less than 10 % and 50 % are required, respectively.

### 3. THERMAL-LENSING EFFECTS IN A MIRROR SUBSTRATE

An optical cavity stores a circulating power which is approximately the finesse times the incident power. In advanced interferometric gravitational wave detectors, a cw optical power of 100 watt from a  $TEM_{00}$  mode single-frequency laser will be coupled into an optical mode-cleaner cavity. The transmitted spatially filtered  $TEM_{00}$  eigenmode will then be coupled into the interferometer. Because of the high internal circulating power on resonance, an absorption loss on the HR coating of the mirror substrates in the mode-cleaner cavity will lead to heating of the mirror. Low-loss mirrors have a total losses (include scattering and absorption losses) less than 100 ppm. Even at 100 ppm, thermal

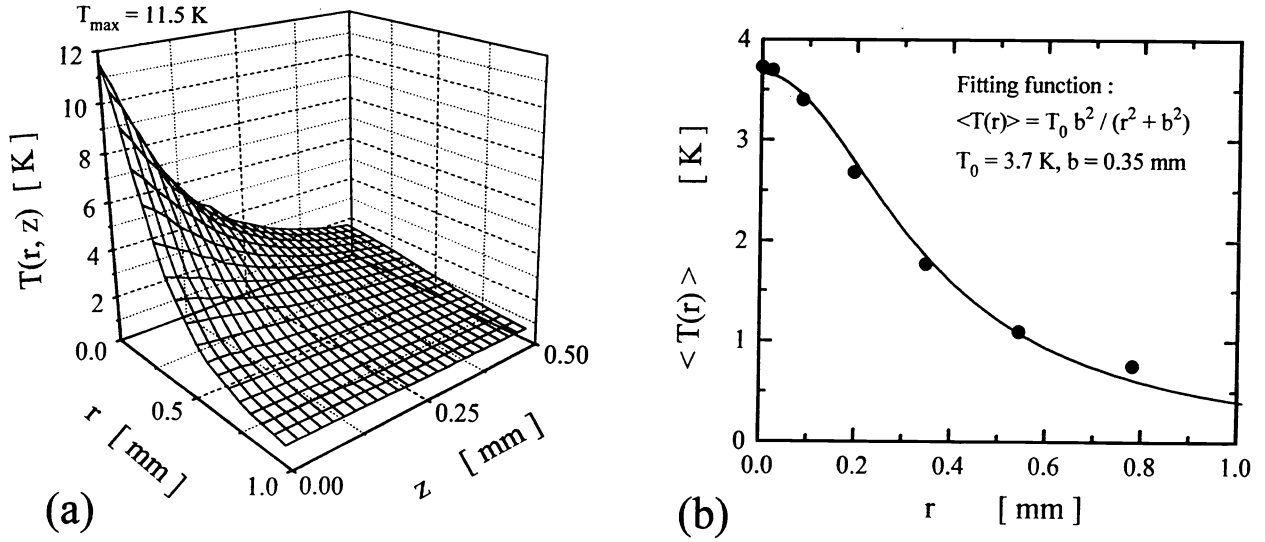


Figure 2: (a) The calculated two dimensional temperature profile in a fused silica mirror substrate and (b) the average temperature profile along the  $z$  axis. Cylindrical mirror size is assumed ( $\phi$ ) 25 x ( $L$ ) 6 mm<sup>3</sup>. The heat source has a Gaussian profile with a beam radius ( $W$ ) of 0.37 mm, a total heat power ( $Q$ ) of 10 mW, and an absorption coefficient ( $\alpha$ ) of 2000 /cm, respectively. Absorption depth corresponds to 5  $\mu$ m. A radiative boundary condition is assumed at all surfaces.

effects in the mirror substrate are not negligible in the gravitational wave detectors. Temperature gradients in the mirror cause a deformation of the mirror substrate which results in a change of the mirror radius of curvature through the thermal expansion.

In this section, we analyze the thermal effects in a ring mode-cleaner cavity. In the model, we assume (1) an isotropic medium with cylindrical symmetry and (2) the boundary condition is that of a radiative cooling between the surfaces of the mirror and air. The two dimensional thermal conductivity equation in steady state and cylindrical coordinate is given by;

$$\left[ \frac{\partial^2}{\partial r^2} + \frac{1}{r} \frac{\partial}{\partial r} + \frac{\partial^2}{\partial z^2} \right] T(r, z) + \frac{Q(r, z)}{k} = 0 \quad (15)$$

where  $k$  and  $Q(r, z)$  are thermal conductivity of the medium in units of W/m/K and the generated heat density in units of W/m<sup>3</sup>. The heat source is assumed to be a Gaussian profile expressed as

$$Q(r, z) = \frac{2Q\alpha}{\pi W^2} \exp \left\{ -2 \frac{r^2}{W^2} - \alpha z \right\} \quad (16)$$

where  $Q$ ,  $W$  and  $\alpha$  are total heat power, beam radius, and absorption coefficient, respectively. To treat surface heating in the 5  $\mu$ m HR coating multilayers, a non-uniform mesh size proportional to  $z^n$  is used in a finite-element analysis. The fused silica substrate is 25 mm in diameter ( $\phi$ ) and 6 mm long ( $L$ ). Heat source has a beam radius based on the cavity-fundamental mode of 0.37 mm, a total heat power of 10 mW, and an absorption coefficient of 2000 /cm which corresponds to an absorption length of 5  $\mu$ m. The absorption length is based on ten stacks of HL (high index layer/low index layer)  $\lambda/4$  multilayers at 1  $\mu$ m.

Figure 2 shows a calculated temperature profile in the fused silica substrate. Fig. 2 (a) and (b) show the two dimensional temperature profile and an averaged temperature profile along the  $z$  axis, respectively. Node numbers in  $r$  and  $z$  axes are 25. The mesh size along the  $r$  and  $z$  axes is proportional to  $r^2$  and  $z^3$ , and the minimum mesh size ( $Dr \times Dz$ ) at  $r = z = 0$  is 22  $\mu$ m x 0.43  $\mu$ m. This mesh size (0.43  $\mu$ m) along the  $z$  axis is small compared to 5

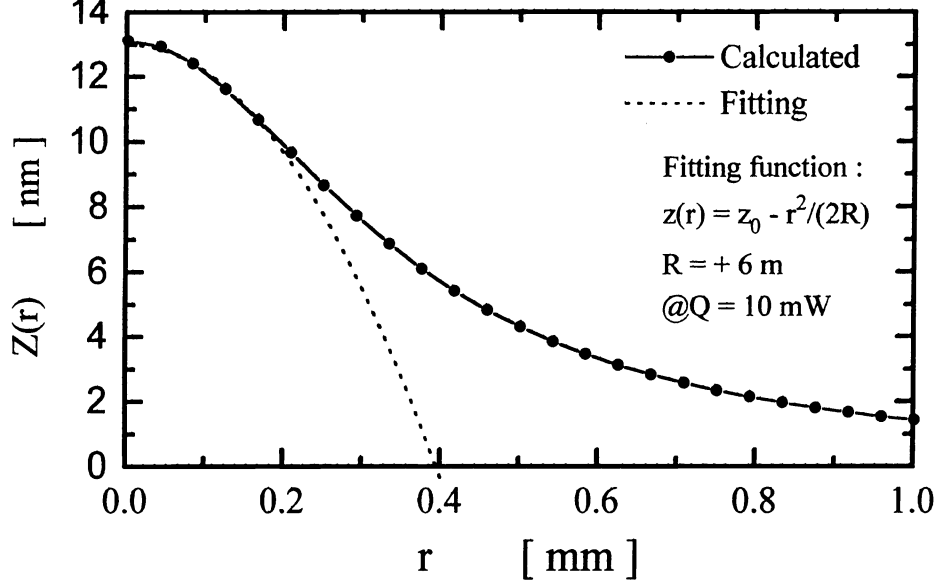


Figure 3: Calculated thermal expansion in the  $z$  axis in a fused silica flat mirror substrate. The dots show the calculated surface profile at the front side of the mirror for a total heat power of 10 mW. The dashed line shows a fit to a parabolic profile. The fitting function corresponds to an effective curvature of + 6 m in convex.

$\mu\text{m}$  absorption length. Boundary condition is that of a radiative cooling between the medium and air with a surface heat transfer coefficient of  $h = 10^{-3} \text{ W/cm}^2/\text{K}$  at all surfaces[12]. The temperature at infinity is assumed to be zero. In the Fig. 2 (a) a maximum temperature of 11.5 K appeared at the center of the mirror front surface. When this temperature profile is resampled with a uniform mesh, the temperature profile was well fit with a Lorentzian function defined by  $\langle T(r) \rangle = T_0 b^2 / (r^2 + b^2)$  where  $T_0$  and  $b$  are 3.7 K and 0.35 mm, respectively as shown in Fig. 2 (b). This fitting function is used to calculate a thermal-induced radius of curvature.

Thermal expansion along the  $z$  axis causes mirror deformation leading to a change of mirror curvature. In a curved mirror, the change of mirror curvature is given by

$$dR = \frac{2R^2}{(\phi/2)^2} (1 + \nu) \alpha_T \langle T(r=0) \rangle L \quad (17)$$

where  $R$  and  $dR$  are the initial mirror curvature and the small change, respectively.  $\langle T(r) \rangle$  and  $\alpha_T$  are average temperature along the  $z$  axis and the thermal expansion coefficient in units of 1/K, respectively. These thermal parameters are summarized in table 1. The mirror distortion was calculated to be  $dR/R = 0.15 \%$  when the total heat power is 10 mW and the initial concave mirror curvature is 1000 mm. For a flat substrate, this equation can not be used. However the thermal-induced lensing effect can be fit with the mirror-surface profile. The mirror-surface profile in the  $z$  axis is given by

$$z(r) = (1 + \nu) \alpha_T \langle T(r) \rangle L. \quad (18)$$

Figure 3 shows a mirror-surface profile  $z(r)$  at a total heat power of 10 mW. The profile is fit with a parabolic function defined by

$$z(r) = z_0 - \frac{r^2}{2R} \quad (19)$$

where  $R$  is the effective mirror curvature. In Fig. 3, the dashed line shows a fitting function with  $R = +6 \text{ m}$ . Since the cavity fundamental mode radius is 0.37 mm, high-order wavefront distortion is expected for  $r \geq 0.25 \text{ mm}$  which can be measured in terms of the mode-coupling efficiency.

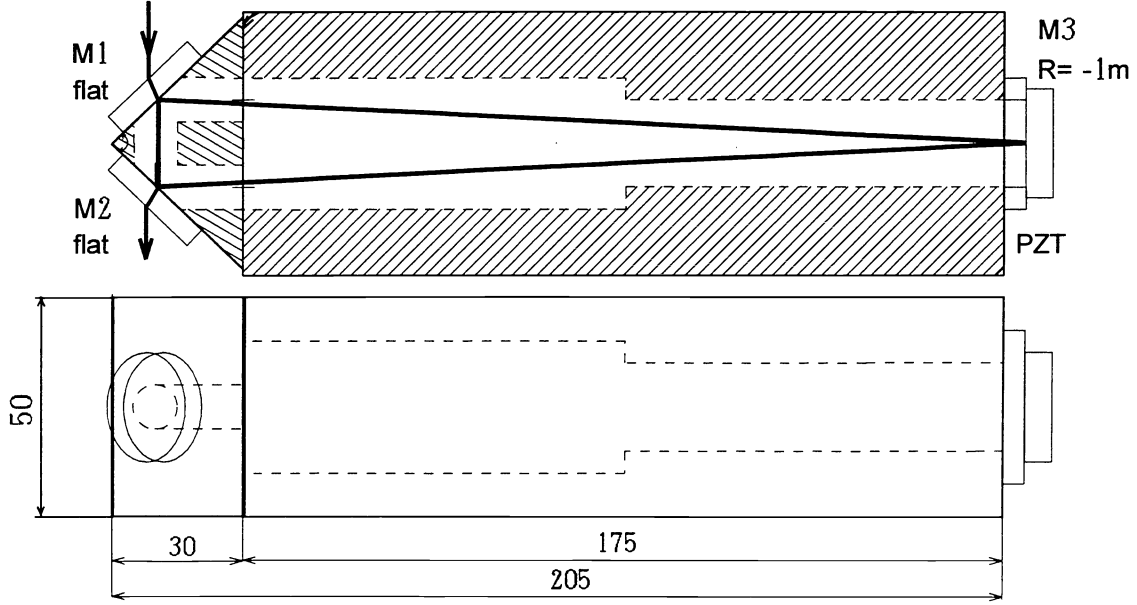


Figure 4: Schematic of the ring mode-cleaner cavity. The ring cavity consists of two flat mirrors ( $M_1$ ,  $M_2$ ) and a one meter curved concave mirror ( $M_3$ ) made of fused silica. The distance between  $M_1$  to  $M_2$  is 20 mm and  $M_1$  to  $M_3$  is 200 mm.

The wavefront of the transmitted beam from the cavity is distorted by thermal-induced optical-path difference (OPD) in the output mirror. Optical-path difference between  $r = 0$  and  $r = \infty$  for a single path is given by

$$OPD = \left[ \frac{dn}{dT} + (n - 1)(1 + \nu)\alpha_T \right] \langle T(0) \rangle L \quad (20)$$

where  $n$ ,  $dn/dT$ , and  $\nu$  are the refractive index of the medium, the linear temperature coefficient, and the Poisson's ratio.

### 3.1. THERMAL-LENSING EFFECTS IN THE RING MODE-CLEANER CAVITY

The ring mode-cleaner shown in Fig. 4 consists of two flat and one 1 meter fused silica mirrors. The distance between  $M_1$  to  $M_2$  and  $M_1$  to  $M_3$  are 20 mm and 200 mm, respectively. The cavity fundamental eigenmodes in the horizontal ( $x$ ) and the vertical ( $y$ ) directions are calculated to have beam-waist radii of  $W_{xe0} = 0.3714$  mm and  $W_{ye0} = 0.3716$  mm. These beam-waist radii correspond to beam divergences of  $\theta_{xe} = 0.9120$  mrad and  $\theta_{ye} = 0.9113$  mrad.

Figure 5 shows calculated beam-waist radii of the cavity-fundamental mode as a function of total heat power generated in each mirror. The cavity eigenmode was calculated by solving the eigenmode equation including the thermal-distortion of the mirrors. In Fig. 5 the solid line and the dashed line show the beam-waist radii for the horizontal ( $x$ ) and vertical ( $y$ ) axes. The dot dashed line shows the ratio of the beam-waist radii. The output becomes an elliptical beam and the beam divergence also changes as a function of the generated heat. The two flat mirrors become convex mirrors due to the thermal expansion in the beam spot and the eigenmode vanishes at a total heat power of 23 mW where the beam radius goes to infinity.

The mode-decoupling efficiency ( $1 - \kappa_{00}$ ) can be calculated with this result and the measured incident beam parameters discussed in section 5; beam-waist radii  $W_{x0} = 371.1 \mu\text{m}$  and  $W_{y0} = 371.0 \mu\text{m}$ , the relative waist position  $z_x = z_y = 0$  mm. In the calculation, thermal effects are calculated for fused silica (FS), ultralow-expansion ceramic (ULE), and sapphire (SP). The thermal properties of these materials are given in table 1[13],[14].

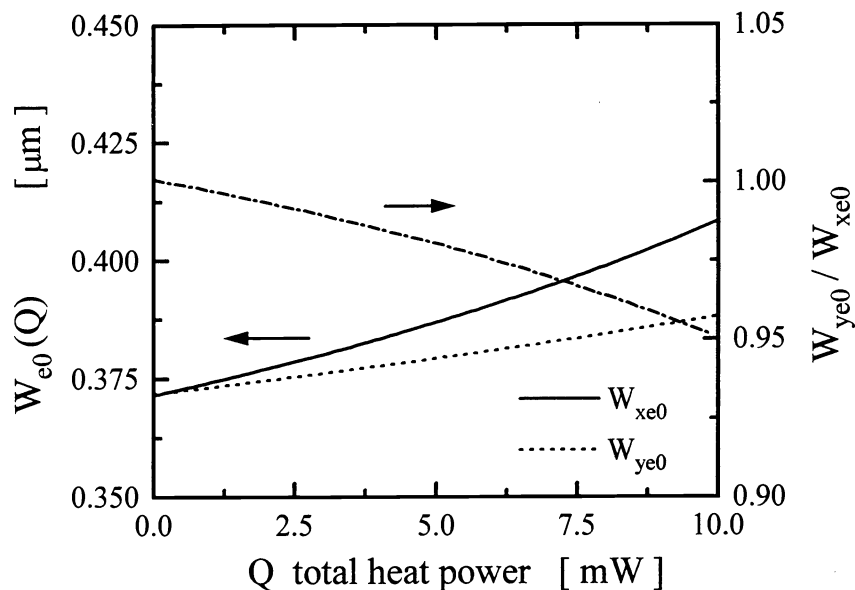


Figure 5: Calculated beam-waist radii of the cavity-fundamental mode as a function of total heat power. Two flat mirrors becomes convex mirrors due to the thermal expansion in the beam spot. The eigenmode vanishes at a total heat power of 23 mW where the beam radius goes to infinity.

Figure 6 shows a calculated mode-decoupling and OPD in the ring mode-cleaner cavity as a function of total heat power in the mirror. In Fig. 6 (a), to achieve a mode-coupling efficiency of 99 % a maximum heat power is determined to be less than 10.5 mW in a fused silica substrate. However, 10.5 mW of total heat power causes an OPD of  $\sim \lambda/4$ . To keep the OPD less than  $\lambda/10$ , the total heat power must be less than 5.3 mW. This heat power corresponds to an internal circulating power of 5.3 kW when the mirror absorption is assumed to be 1 ppm. To identify the critical circulating power, the mirror absorption loss should be evaluated. In the initial LIGO interferometer, a 10 watt TEM<sub>00</sub> single-frequency laser will be injected into the 200 finesse ring mode-cleaner cavity, which results in an internal circulating power of approximately 700 watts. Since this corresponds to a total heat power of 0.7 mW, this heat power will not cause significant thermal distortions.

To discuss a figure of merit of these materials with regard to thermal effects, we define two parameters ( $f_1$ ,  $f_2$ ) using Eqs. (18), (20). Mirror curvature change due to thermal expansion and optical-path difference are proportional

Table 1: Thermal properties of fused silica, ULE, and sapphire.

Materials	$k$ [W/m/K]	$\alpha_T$ [1/K]	$\nu$	$n$ @1.06 $\mu\text{m}$	$dn/dT$ [1/K]
Fused silica	1.38	$5.1 \times 10^{-7}$	0.16	1.45	$1.03 \times 10^{-5}$
ULE	1.31	$1 \times 10^{-8}$	0.17	1.48	$1.07 \times 10^{-5}$
Sapphire	46	$6.77 \times 10^{-6}$	0.23	1.76	$1.23 \times 10^{-5}$

$k$ : thermal conductivity,  $\alpha_T$ : thermal expansion coefficient,  $\nu$ : Poisson's ratio,  $n$ : refractive index,  $dn/dT$ : the linear temperature coefficient.

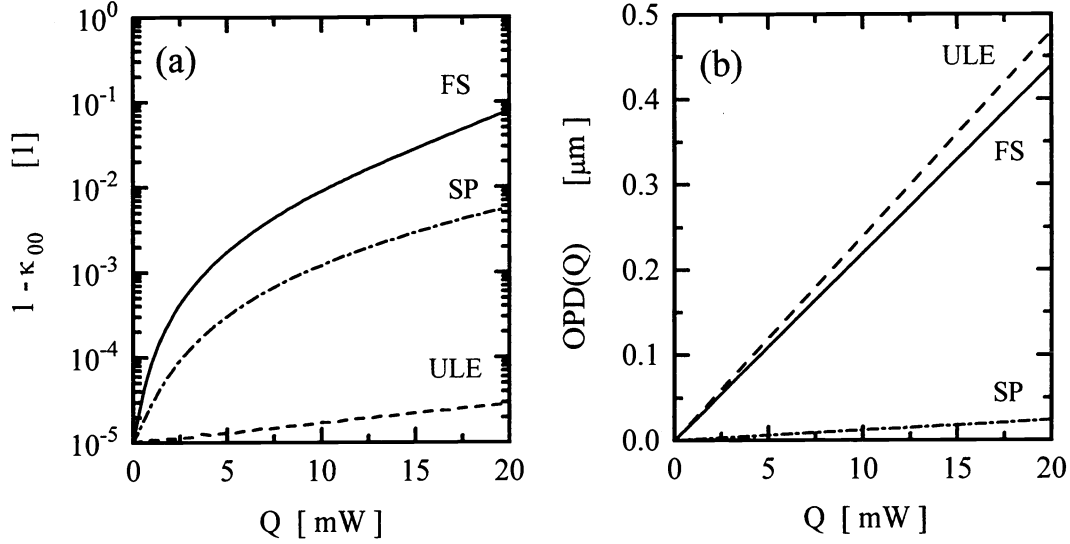


Figure 6: (a) Calculated mode-coupling efficiency and (b) optical-path difference (OPD) as a function of total heat power ( $Q$ ) in fused silica, ULE, and sapphire substrates.

to

$$f_1 = \frac{(1 + \nu)\alpha_T}{k}, \quad (21)$$

$$f_2 = \frac{dn/dT + (n - 1)(1 + \nu)\alpha_T}{k} \quad (22)$$

in units of m/W, respectively. A figure of merit of a material is given by the inverse of these parameters. To minimize these thermal effects a small thermal expansion coefficient, a large thermal conductivity, and a small thermal coefficient ( $dn/dT$ ) are desirable. A comparison of fused silica, ULE, and sapphire are summarized in table 2. Here  $f_1$  and  $f_2$  for fused silica are calculated to be  $4.3 \times 10^{-7}$  [m/W] and  $7.7 \times 10^{-6}$  [m/W]. Critical circulating powers  $P_{c1}$  and  $P_{c2}$  are calculated with the parameters  $f_1$  and  $f_2$  to satisfy a mode-coupling efficiency of 99 % and an OPD of  $\lambda/10$  at 1  $\mu\text{m}$ , respectively. Lower critical power gives the practical critical circulating power ( $P_c$ ). Sapphire provides the largest critical power of 25 kW. But, if active-mode coupling control is used to compensate the thermal-induced mode-size mismatching, the critical power is given by  $P_{c2} = 100$  kW by the thermal-induced OPD. In a future advanced mode-

Table 2: Magnitude of thermal effects and critical internal circulating powers in fused silica, ULE, and sapphire.

Materials	$f_1/f_{1(FS)}^1$	$f_2/f_{2(FS)}^2$	$P_{c1}^{3,4}$	$P_{c2}^{3,5}$
Fused silica	1.0	1.0	10.5 kW	5.3 kW
ULE	0.021	1.1	500 kW	4.8 kW
Sapphire	0.42	0.053	25 kW	100 kW

1)  $f_{1(FS)} = 4.3 \times 10^{-7}$  [m/W].

2)  $f_{2(FS)} = 7.7 \times 10^{-6}$  [m/W].

3) Mirror absorption loss of 1 ppm is assumed.

4) Mode-coupling efficiency of 99 % is satisfied.

5) OPD of  $\lambda/10$  at 1  $\mu\text{m}$  is satisfied.



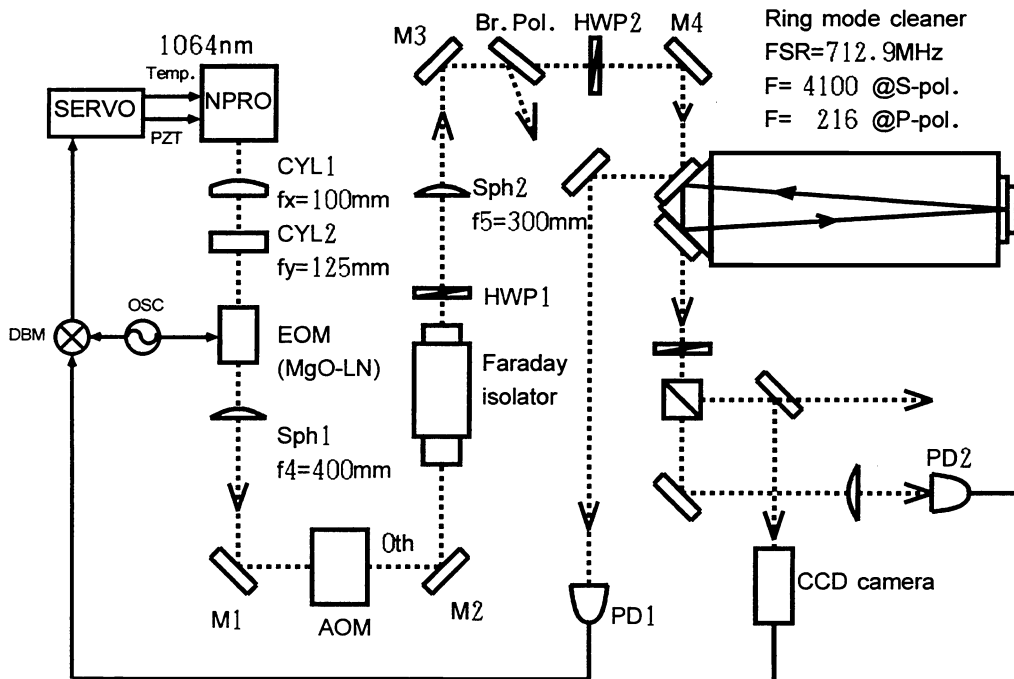


Figure 7: Experimental setup of the mode-coupling experiment with the ring mode-cleaner cavity. CYL; cylindrical lens, SPH; spherical lens, HWP; half-waveplate, Br.Pol.; Brewster angle thin-film polarizer, M ; HR mirror, PD; photodetector, OSC; oscillator, and DBM; double-balanced mixer.

cleaner cavity, sapphire may be required as the mirror substrate. However sapphire is a biaxial birefringence crystal and would require external quarter waveplates at input and output to compensate the polarization of the input beam.

#### 4. EXPERIMENTAL SETUP

The experimental setup used in these experiments is shown in Fig. 7. The laser is a cw TEM<sub>00</sub> mode, single-frequency diode-pumped Nd:YAG laser (NPRO : 122-1064-300F, Lightwave Electronics). The output power and laser wavelength are 326 mW and 1064 nm. Because the output beam is elliptical (1 : 1.3), two cylindrical lens were used to circularize the output beam. A MgO-LiNbO<sub>3</sub> electro-optic modulator (EOM) (4004D, New Focus) is used to generate sidebands for frequency stabilization and to measure the frequency response of the ring mode-cleaner. An acousto-optic modulator (AOM) is used to measure the cavity-decay time of the mode cleaner by ringdown. One of the purpose of this experiment is to measure the laser-beam quality and wavefront distortion caused by optical components in the beam using the mode-coupling efficiency. In a laser, the output beam includes high-order transverse modes due to thermal-induced distortion produced by the optical pumping. Mode-coupling efficiency ( $\kappa_{mn}$ ) to an optical cavity gives us beam-quality information. We can measure how much power is coupled into a TEM<sub>mn</sub> mode. Because an optical cavity provides a complete set of eigenmodes, one can analyze a laser-beam quality precisely.

The ring mode-cleaner mirrors are glued on a fused silica spacer and a piezo-electric transducer (PZT) is between the spacer and the curved mirror. The incident angle on the flat mirrors are 43.6 degrees and on the curved mirror is 2.9 degrees. These mirrors were made by Research-Electro Optics in Boulder CO. The ring mode cleaner has two independent eigen-polarizations; *p* polarization and *s* polarization. The flat mirrors have an intensity reflectance of 98.56 % in *p* polarization and 99.92 % in *s* polarization. The curved mirror has a reflectance of more than 99.997 %

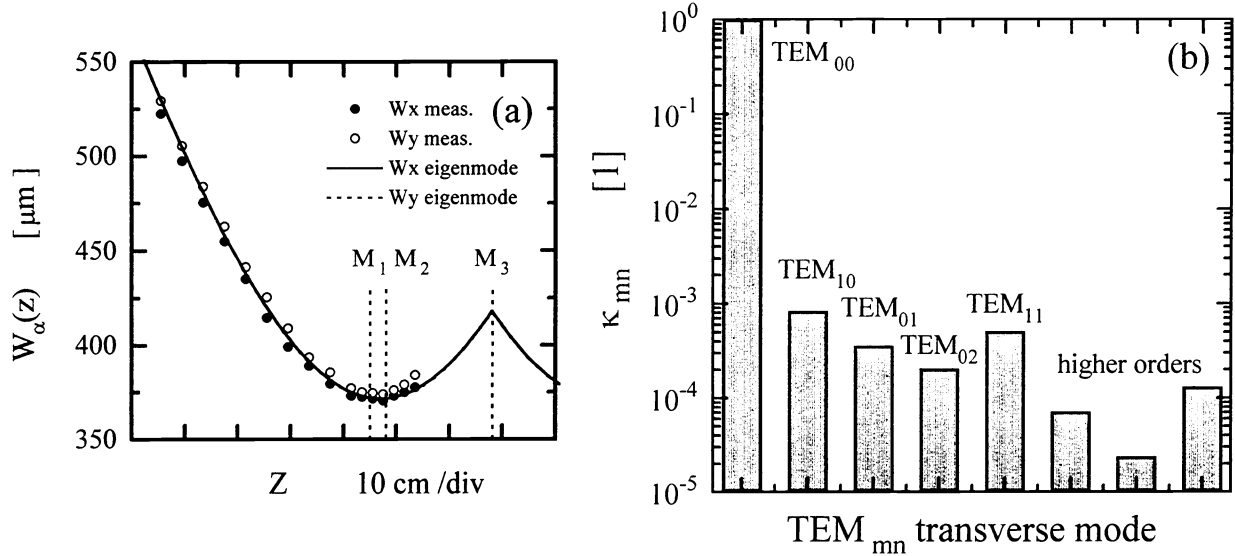


Figure 8: (a) Focusing-beam propagation around beam waist for the ring mode-cleaner cavity. Closed dots and open dots are measured in the  $x$  and  $y$  axes. The solid line and dashed line shows the cavity fundamental eigenmodes along the  $x$  and  $y$ . (b) Mode-coupling efficiency for each transverse eigenmode. The incident power is 2 mW and the polarization is  $p$  polarization. Cavity FSR and the finesse in  $p$  polarization are 712.9 MHz and 216. A mode-coupling efficiency ( $\kappa_{00}$ ) to the cavity fundamental mode of 99.8 % was achieved.

for both polarizations.

## 5. MODE-COUPLING EXPERIMENT WITH THE RING MODE CLEANER

The laser beam parameters were precisely measured and lens positions were adjusted using measurements with a beam analyzer (BeamScan, Photon Inc.). Figure 8 (a) shows the beam propagation from the laser to the ring mode cleaner. Closed and open dots show the measured beam radii. Solid and dashed line are the cavity eigenmodes in the  $x$  and  $y$  axes, respectively. In the mode-coupling measurement, the ring mode cleaner was inserted at the laser-beam waist to  $\pm 10$  mm.

Figure 8 (b) shows a measured mode-coupling efficiency. The incident power is 2 mW and the polarization is  $p$  polarization for this measurement. A maximum mode-coupling efficiency to the cavity fundamental mode of 99.8 % was achieved. Mode-coupling of each high-order transverse mode was less than 0.1 %. To our knowledge this mode-coupling efficiency is the highest yet obtained. The measured mode-decoupling efficiency ( $1-\kappa_{00}$ ) results from accumulated wavefront distortions caused by the laser cavity, transmission through many optical components (lens, modulators, etc.), and residual misalignment of the mirrors of the ring mode cleaner. Thus, we can say that "99.8 % of the laser output power is in the diffraction-limited  $TEM_{00}$  mode" and "Wavefront distortion caused by optical components are less than 0.2 %".

## 6. SUMMARY

In summary, we have demonstrated the mode-coupling of a diode-pumped Nd:YAG laser to a ring mode-cleaner cavity with 99.8 % efficiency. Mode-coupling of each high-order transverse mode was less than 0.1 %. This is the

highest mode-coupling yet obtained to our knowledge. High-sensitive measurements are expected in the thermal-lensing effect discussed here. Mode-decoupling due to the thermal-lensing effects on the HR coating multilayers in the mode-cleaner cavity were calculated using a finite-element analysis in fused silica, ULE, and sapphire substrates. The ring mode cleaner made of a fused silica substrate can be used at up to a cavity internal power of 5.3 kW with a mode-coupling efficiency of more than 99 % and an optical-path difference in the transmitted beam of less than  $\lambda/10$  at  $1\mu\text{m}$ . However cylindrical symmetry was assumed in the ring mode-cleaner cavity, the elliptical beam spot on the HR mirror will give us slightly smaller thermal-lensing effects than that discussed here. For the advanced gravitational wave detector mode cleaner, sapphire may be required as the mirror substrate to reduce thermal distortions.

## ACKNOWLEDGMENTS

We thank Stan Whitcomb and Rick Savage of the California Institute of Technology for their helpful discussions. This work was supported by the National Science Foundation grant (PYS-9630172) and (PYS-9210038) under cooperative agreement with the LIGO project.

## REFERENCES

- [1] K. S. Thorne, "300 Years of Gravitation," S. W. Hawking and W. Israel eds., Cambridge U. Press, Cambridge, pp. 330 - 458, 1987.
- [2] A. Abramovici, W. E. Althouse, R. W. P. Drever, Y. Gürsel, S. Kawamura, F. J. Raab, D. Shoemaker, L. Sievers, R. E. Spero, K. S. Thorne, R. E. Vogt, R. Weiss, S. E. Whitcomb, and M. E. Zucker, "LIGO: the laser interferometer gravitational-wave observatory," *Science* **256**, pp. 325 - 333, 1992.
- [3] R. L. Byer, "GALILEO: Stanford Advanced Gravitational-Wave Laser Interferometer Program," Proposal to the National Science Foundation, 1995 December 20.
- [4] N. Uehara, A. Ueda, K. Ueda, H. Sekiguchi, T. Mitake, K. Nakamura, and N. Kitajima, and I. Kataoka, "Ultralow-loss mirror of the parts-in- $10^6$  level at 1064 nm," *Opt. Lett.* **20**, pp. 530 - 532, 1995.
- [5] P. Hello and J-Y. Vinet, "Analytical models of transient thermoelastic deformations of mirrors heated by high power cw laser beam," *J. Phys. France* **51**, pp. 2243 - 2261, 1990.
- [6] W. Winkler, K. Danzmann, A. Rüdiger, and R. Shilling, "Heating by optical absorption and the performance of interferometric gravitational-wave detectors," *Phys. Rev. A* **44**, pp. 7022 - 7036, 1991.
- [7] N. Uehara and K. Ueda, "Accurate measurement of ultralow loss in a high-finesse Fabry-Perot interferometer using the frequency response functions," *Appl. Phys. B*, **61**, pp. 9-15, 1995.
- [8] N. Uehara and K. Ueda, "Accurate measurement of the radius of curvature of a concave mirror and the power dependence in a high-finesse Fabry-Perot interferometer," *Appl. Opt.* **34**, pp. 5611 - 5619, 1995 .
- [9] H. Kogelnik, "Coupling and conversion coefficients for optical modes," *Symposium on Quasi-Optics*, pp 333 - 347, 1964.
- [10] A. Yariv, "Optical Electronics," 3rd edn. NY, CBS College Publishing, Chap. 4., 1985.
- [11] A. E. Siegman, "Lasers," University Science, Mill Valley, CA, 1986.

- [12] E. R. G. Eckert and R. M. Drake, Jr., "Analysis of Heat and Mass Transfer," 2nd ed. New York, McGraw-Hill, 1972.
- [13] R. Waynant and M. Ediger, "Electro-optic handbook," chap. 11, McGraw-Hill Inc, New York, 1994.
- [14] Corning code 7971, Titanium silicate, (MP-21-4, Corning, NY 14831), 1990.